Exploring parameter constraints on quintessential dark energy: The exponential model

Brandon Bozek, Augusta Abrahamse, Andreas Albrecht, and Michael Barnard
Physics Department, University of California, Davis, California, USA
(Received 17 January 2008; published 5 May 2008)

We present an analysis of a scalar field model of dark energy with an exponential potential using the Dark Energy Task Force (DETF) simulated data models. Using Markov Chain Monte Carlo sampling techniques we examine the ability of each simulated data set to constrain the parameter space of the exponential potential for data sets based on a cosmological constant and a specific exponential scalar field model. We compare our results with the constraining power calculated by the DETF using their "$w_0 - w_a$" parametrization of the dark energy. We find that respective increases in constraining power from one stage to the next produced by our analysis give results consistent with DETF results. To further investigate the potential impact of future experiments, we also generate simulated data for an exponential model background cosmology which cannot be distinguished from a cosmological constant at DETF "Stage 2," and show that for this cosmology good DETF Stage 4 data would exclude a cosmological constant by better than 3σ.

DOI: 10.1103/PhysRevD.77.103504 PACS numbers: 95.36.+x, 98.80.Es

I. INTRODUCTION

In the late 90's, two independent teams presented evidence from supernova observations that the universe, instead of slowing down due to gravity, is accelerating [1,2]. In the standard cosmological framework, the acceleration is caused by a mysterious new form of matter, dubbed "dark energy," that makes up roughly 70% of the universe. There is a wide variety of possible explanations for dark energy. The simplest model that provides a good fit to the data is a cosmological constant. A cosmological constant is equivalent to a homogeneous fluid with a constant energy density and a ratio of pressure to energy density (the "equation of state parameter" w), equal to -1 at all times. Yet, despite compelling evidence for the existence of dark energy, it is unclear whether the dark energy density is constant or varies with time. There are many different proposals for a dynamical form of dark energy, one of them being quintessence. Quintessence describes the acceleration being caused by a scalar field, ϕ, but even just among quintessence models there is a tremendous variety of possible behaviors. There is considerable interest in acquiring better data in order to improve our understanding of dark energy.

Recently the Dark Energy Task Force (DETF) released a report charting a course for future experiments [3]. They modeled dark energy as a homogeneous and isotropic fluid with an equation of state parametrized by $w(a) = w_0 + w_a(1 - a)$, where the scale factor $a = 1$ today. Defining Stage 1 to be what is already known, they forecasted data for three additional experimental stages: Stage 2 data represents on-going experiments that will be completed in the near future. Stage 3 data sets represent medium sized proposed experiments. Last, Stage 4 data sets represent proposed large scale future space and ground-based experiments. Each stage is further categorized as either "optimistic" or "pessimistic" depending on how well the systematics are expected to be constrained. The scientific impact of a stage was quantified in terms of a "figure of merit" (FoM). The figure of merit is defined to be the ratio of the area of the 2σ contour of the $w_0 - w_a$ space for Stage 2 divided by the area of the 2σ contour of the $w_0 - w_a$ space for Stage 3 (or 4).

The DETF analysis leaves several open questions, some of which our research seeks to address. The $w_0 - w_a$ parametrization is not motivated by a physical model of dark energy and provides cosmological solutions that may be very different from a scalar field model. As illustrated in Fig. 1, the w curves generated by the exponential scalar field model that we consider in this paper are not especially well fit by curves in the $w_0 - w_a$ family, except for those nearly identical to $w = -1$. Thus the relationship between the DETF results and the impact of future experiments on scalar field models is not clear. A good way to clarify this point is to model the impact of future data sets directly on particular scalar field quintessence models, which is what we do here. Our work complements the DETF report as well as work by other authors using alternative $w(a)$ parametrizations [4,5], parametrizations of ρ_{DE} [6], and model independent scalar field parameters [7].

The exponential scalar field model has been used in many different cosmological contexts due to its ability to give scaling solutions for the scalar field energy density ρ_ϕ where $\frac{d(\log(\rho_\phi))}{d(\log(a))} \rightarrow \beta$. The constant β depends on parameters in the scalar field potential as well as the other forms of matter present in the universe. Originally the potential was used for power law inflation models and was shown to have a range of attractor solutions [8]. Its ability to produce attractor solutions that scale like the background energy density made it an interesting choice for a dark matter candidate [9–11]. The variety of scaling solutions is well

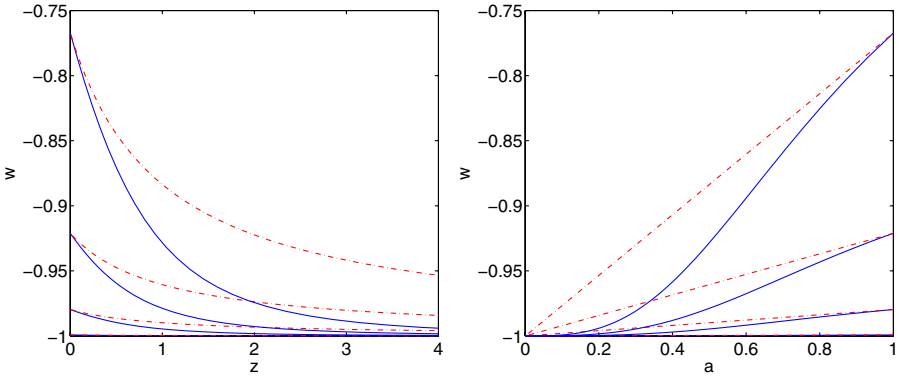

FIG. 1 (color online). Here we illustrate the differences between $w(a)$ curves from the exponential model (solid line) and from the ansatz used by the DETF (dot-dashed line). Curves are plotted with respect to z (left panel) and a (right panel). The four curves from top to bottom are given by (w_0, w_a): $(-0.77673, -0.2327)$, $(-0.9211, -0.0789)$, $(-0.9797, -0.0203)$, $(-0.9992, -0.0008)$. Using the final parametrization (explained in Sec. III), the exponential model parameters are given by (λ, V_I): (0.07, 0.3725), (0.35, 0.42), (0.7, 0.42), (1.2, 0.52) (in units defined in the text). Both models give $w(a = 1)$ to be the same value for each set of curves and $w(a_I) = -1$ for all curves shown.

covered by Copeland, *et al.* [12] where they argue that consideration of "fine-tuning" parameters and constraints from nucleosynthesis give $\lambda > 20$ as a natural choice. This range of λ values would not allow for late time cosmological acceleration and is therefore ruled out as an explanation for dark energy. The fine-tuning that is required to successfully describe dark energy with this model is needed so that the scalar field energy density can be initially very small; of the order of the dark energy density today. This has caused this model to be discarded by many authors on the basis that the model has lost the theoretical generality that made the potential initially interesting. However, as a practical matter the fine-tuning is straightforward to implement, and the potential is very simple and easy to work with. Because of this simplicity, we found it valuable to have this potential as part of our larger project (which includes a variety of more complicated quintessence potentials [13,14]). The simplicity helped us deal with a number of technical issues first with the exponential model and then transfer our understanding to the more complicated cases. In addition, realistic cosmologies for the exponential model have their special forms for $w(a)$ (illustrated in Fig. 1). We found it useful to include this family of $w(a)$ curves in our set of possibilities to more fully understand the constraining power of future data sets.

The paper is organized as follows. In Sec. II we provide an introduction to our scalar field model and its cosmological solutions. In Sec. III we describe how we come about our choice of parametrization, as this is a critical step in the MCMC analysis. (An account of our general MCMC methods and data modeling can be found in the appendix of our companion paper [13]. This paper contains only information specific to the exponential model.) Section IV presents our results for data simulated using a background cosmology with a cosmological constant and then Sec. V presents results where the data is based on a cosmology with exponential model quintessence. Finally, we summarize our key results in the conclusions.

II. EXPONENTIAL MODEL COSMOLOGY

We model dark energy as a homogeneous scalar field evolving in an exponential potential

$$V = V_0 e^{-\lambda\phi}. \tag{1}$$

The cosmological evolution of this scalar field in a Friedmann-Robertson-Walker (FRW) universe is then given by solving:

$$\frac{d^2\phi}{dt^2} + 3H\frac{d\phi}{dt} + \frac{dV(\phi)}{d\phi} = 0, \tag{2}$$

$$H^2 = \frac{1}{3M_p^2}(\rho_r + \rho_m + \rho_\phi) - \frac{k}{a^2}, \tag{3}$$

$$\rho_\phi = \frac{1}{2}\left(\frac{d\phi}{dt}\right)^2 + V(\phi), \tag{4}$$

where M_p is the reduced Planck mass. The equation of state of the scalar field is given by

$$w = \frac{\frac{1}{2}(\frac{d\phi}{dt})^2 - V(\phi)}{\frac{1}{2}(\frac{d\phi}{dt})^2 + V(\phi)}, \tag{5}$$

which we will use in discussing an evolving dark energy. In this picture a cosmological constant is equivalent to a scalar field with $w = -1$.

In our analysis we initially set $\frac{d\phi}{dt} = 0$ [15]. This leaves the dynamics of the field completely determined by the slope and curvature of the potential:

$$\frac{dV}{d\phi} = -\lambda V_0 e^{-\lambda\phi}, \qquad \frac{d^2V}{d\phi^2} = \lambda^2 V_0 e^{-\lambda\phi}. \tag{6}$$

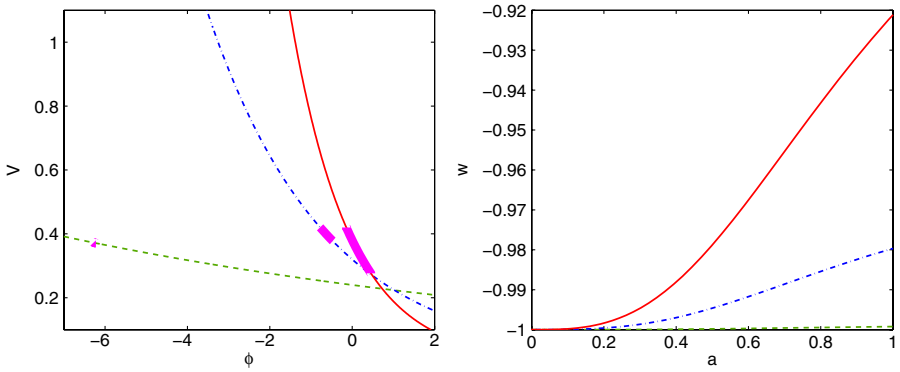

FIG. 2 (color online). The left panel shows three examples of the exponential potential (dashed line: $\lambda = 0.07$, $V_0 = 0.24$, $\phi_I = -6.28$, long-short dashed line: $\lambda = 0.35$, $V_0 = 0.32$, $\phi_I = -0.78$, solid line: $\lambda = 0.7$, $V_0 = 0.38$, $\phi_I = -0.14$. V_0 is given in units of h^2, as mentioned in Sec. IV). The path of the scalar field is depicted by thick solid curves. The corresponding w behavior is shown in the right panel. The solid curve gives the potential used for the fiducial model discussed in Sec. V.

Since the initial field velocity is zero, the initial equation of state is $w = -1$, mimicking a cosmological constant. As the field begins to roll the equation of state begins to depart from -1. The rate of this departure is determined by the steepness of the potential. A steeper slope gives changes in ϕ that correspond to larger changes in w. Likewise, a flat slope gives little change in ϕ and therefore has a cosmology similar to a cosmological constant, as shown in Fig. 2.

The possible scaling solutions achievable by the exponential model are systematically discussed by Copeland, *et al.* [12]. If a scaling solution is reached before the onset of dark energy domination the universe will not accelerate and therefore is a poor match to current data. However, there are subsets of scaling solutions that reach their scaling solution after dark energy domination and provide different fates for the universe. These scaling solutions fall into two categories: (i) $0 < \lambda < \sqrt{2}$ or (ii) $\sqrt{2} \leq \lambda < \lambda_*$. Solutions with λ values in category (i) approach scaling where $w \rightarrow \frac{\lambda^2}{3} - 1$, giving late time acceleration. For category (ii), we define λ_* to be the value that gives $w(a = 1) = -\frac{1}{3}$, but the scaling solution leads to $w(a > 1) > -\frac{1}{3}$. It is possible for λ_* to be larger than $\sqrt{3}$ and therefore have $w(a > 1) \rightarrow 0$. This value depends on the initial scalar field energy density, $\rho_{\phi,I}$, which in turn determines when the field begins to approach its scaling solution, i.e., when the field starts rolling. We are allowing $\rho_{\phi,I}$ and other cosmological parameters to float so a universal value of λ_* cannot be uniquely determined.

III. PARAMETRIZATION

In order to run our MCMC analysis on the potential $V = V_0 e^{-\lambda\phi}$, we first need to make a careful choice of parameters. The obvious choice of the potential parameters V_0, λ, and the initial field value ϕ_I presents several problems. Rewriting the potential $V = V_0 e^{-\lambda\phi} \rightarrow V = e^{\ln(V_0) - \lambda\phi}$ reveals a degeneracy between $\ln(V_0)$ and $\lambda\phi_I$. For fixed values of λ, a change in ϕ_I and a corresponding change in $\ln(V_0)$ gives identical cosmological solutions. This will lead to an unconstrained and uninteresting parameter space. Fixing V_0 removes this degeneracy. We make the choice of $V_0 = \rho_\Lambda = 8.74 \times 10^{-121}$ (in reduced Planck units), which is the value of the cosmological constant energy density used by the DETF. This is the simplest choice, although not absolutely necessary. Other choices of V_0 would provide equivalent cosmological solutions.

Removing the degeneracy and fixing V_0 leaves λ and ϕ_I as the two model parameters. However, this choice leads to an "infinite direction" in $\lambda - \phi_I$ space: Since the data for the first part of our analysis is modeled on a cosmological constant, the most probable values of λ are those where λ approaches zero. As λ approaches zero, ϕ_I can take any value and produce solutions indistinguishable from a cosmological constant. This leads to an infinite unconstrained direction in parameter space that is uninteresting and also fatal to the MCMC techniques.

One can resolve this problem by placing a bound on λ or ϕ_I. For small values of λ, a bound placed on λ is nearly equivalent to placing a bound on $w(a = 1)$. A choice of a bound on λ can be chosen such that the difference from $w = -1$ is small, however, the choice is arbitrary. Further, for data based on a Λ universe, the closer the bound is placed to $\lambda = 0$, the more the allowed region of parameter space squeezes against this bound as smaller values of λ allow a wider range of ϕ_I, basically partially restoring the degeneracy we are trying to eliminate. This arbitrariness and distortion of allowed parameter ranges make bounding λ a poor choice for addressing the parameter space degeneracies in this model. The squeezing effect leads to incorrect conclusions about allowed values of λ. The space appears to disfavor larger values of λ, or equivalently larger departures from $w(a = 1) = -1$, than would the space in the final parametrization that we discuss next.

We find the best choice of free model parameters to be V_I, where $V_I = V(\phi_I)$, and λ. The value of ϕ_I is then determined from λ and V_I. This parametrization avoids the

degeneracy discussed in the previous paragraph since a cosmological constant of a particular value is only represented at one point ($V_I = \rho_\Lambda$ and $\lambda = 0$) in the $\lambda - V_I$ space. Values similar to a cosmological constant are explored without an arbitrary bound placed on any parameter. This allows the MCMC method freedom to explore a more natural space.

There is no loss of generality with this choice of parametrization as is easily seen by the slope and curvature of the potential in the new parameters:

$$\frac{dV}{d\phi} = -\lambda V_I, \qquad \frac{d^2V}{d\phi^2} = \lambda^2 V_I. \tag{7}$$

This parametrization allows a simple intuition about the role of these parameters forming the solutions. Small values of λ give a flat potential and the scalar field will be stationary, independent of the choice of V_I. For large values of λ the field will roll and the amount to which it does will depend on the value of V_I.

IV. COSMOLOGICAL CONSTANT FIDUCIAL DATA

With our parametrization firmly in hand, we now analyze the DETF data sets based on a cosmological constant cosmology using the MCMC technique. The likelihood contours for Stage 2, Stage 3 Photo Optimistic, Stage 4 Ground LST Optimistic, and Stage 4 Space Optimistic are shown in Fig. 3 for the $\lambda - V_I$ space. In all plots shown in this paper we use the DETF supernova, weak lensing, baryon oscillation, and PLANCK (using the alternate parameters as in [5]) data sets but not the cluster data sets due to technical problems adapting the DETF cluster data models to our methods. These technical problems are similar to those outlined in [5], where similar issues were encountered. Our plots were constructed by marginalizing over all the cosmological parameters, ω_m, ω_k, ω_B, δ_ζ, n_s, the various nuisance parameters, and/or the photo-z parameters. The nuisance and photo-z parameters are detailed in the appendix of one of our companion papers [13]. The fiducial values for the cosmological parameters are shown in Table I. The values for all energy densities and V_I in the remainder of the paper are in units of h^2, where $h = \frac{H}{100}$.

Figure 4 gives likelihood contours in $\lambda - \delta\omega_{\rm DE}$ space, where $\delta\omega_{\rm DE} \equiv \omega_{\rm DE}(a = 1) - \omega_{\rm DE}(a_I)$. Here $\omega_{\rm DE} = \frac{\rho_\phi}{\rho_c} h^2$ and $\rho_c = 3M_p^2 H^2$. The value of $\delta\omega_{\rm DE}$ gives the amount the dark energy density has changed since the simulation started at scale factor a_I (well in the radiation era). Values of $\delta\omega_{\rm DE}$ different from zero correspond to dynamical dark energy. Figure 5 shows an enlarged version of the $\lambda - \delta\omega_{\rm DE}$ space for Stage 3 and Stage 4 experiments.

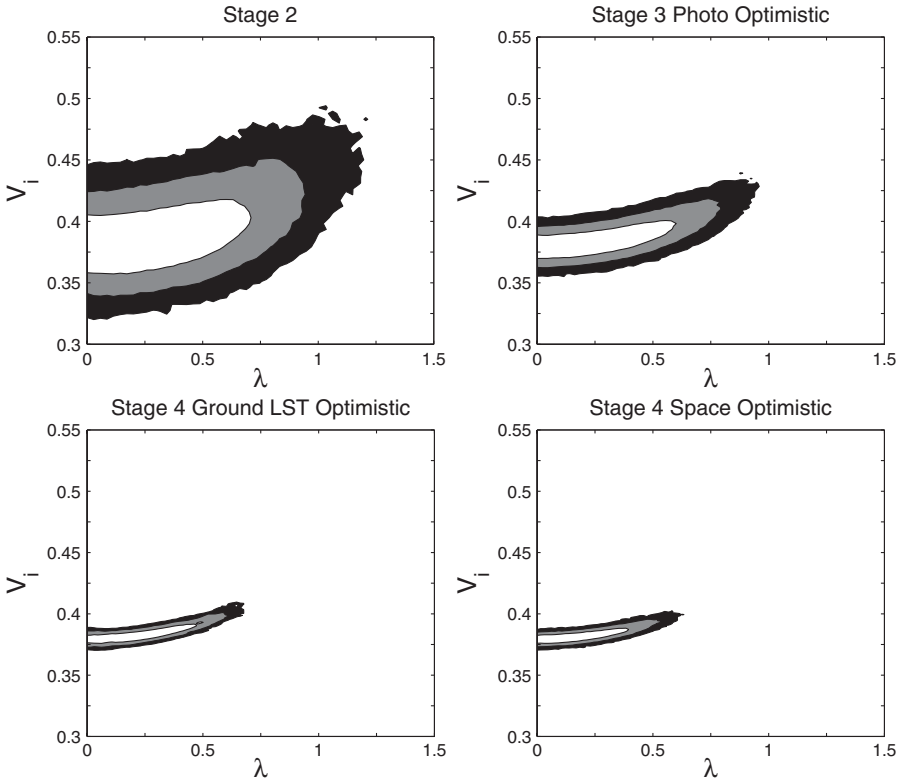

FIG. 3. Likelihood contours in the $V_I - \lambda$ space for cosmological constant data models. The three contours give 68.27%, 95.44%, and 99.73% confidence regions.

TABLE I. ΛCDM (left column) and exponential (right column) fiducial parameter values. The nuisance and photo-z parameters are 0. $\omega_{\rm DE}$ is the same as V_I for a ΛCDM universe and $\omega_{\rm DE} = 0.372$ for the exponential universe displayed in the right column, although it is not a parameter varied for either fiducial model.

ω_m	0.146	0.146
ω_k	0.0	0.0
ω_B	0.024	0.024
n_s	1.0	1.0
δ_ζ	0.87	0.87
λ	0.0	0.7
V_I	0.3796	0.42

For Stage 2, values of λ from 0 to about 0.15 in Fig. 4 correspond to shallow slopes and do not allow for much change in the amount of dark energy. For these values of λ there is a spread in V_I in the $\lambda - V_I$ space (Fig. 3). Since these values are consistent with a nonevolving dark energy, the spread in V_I is essentially a measure of how well the experiment is measuring $\omega_{\rm DE}(a = 1)$. Values of $\lambda > 0.15$ all correspond to detectable differences from a cosmological constant. This portion of the $\lambda - V_I$ space has an upturned feature. As the slope gets steeper the field needs to start higher up in the potential in order to roll down to acceptable values of $\omega_{\rm DE}(a = 1)$. These features are evident in the plots for Stage 3 and Stage 4, although by Stage 4 it is less clear as the parameter space has shrunken to values closer to a cosmological constant, and so the upturned trend has diminished.

Comparing Stage 2 to Stage 3 Photo Optimistic, and then on to Stage 4, there is a significant tightening of the allowed area in parameter space. This increased constraining power is similar to the factors of about three (Stage 2 to Stage 3) and ten (Stage 2 to Stage 4) increase in constraining power noted by the DETF in the $w_0 - w_a$ space. The $\lambda - \delta\omega_{\rm DE}$ contours in Fig. 4 allow one to interpret the constraining power already seen in the $\lambda - V_I$ space in terms of a specific aspect of the dark energy dynamics, namely, the overall change in dark energy density (given by $\delta\omega_{\rm DE}$).

Figure 6 shows plots of the allowed functions of $w(z)$ for each data set. The plots are constructed by selecting around 100 points taken uniformly within the 3σ contour (thus also including points within the 1 and 2σ contours). This is done to illustrate the full range of solutions not excluded at better than 3σ. The furthest most curve from $w = -1$ for each stage corresponds to the top right most tip in the $\lambda - V_I$ space.

Since we are interpreting the data using the exponential quintessence model, we can use our knowledge of how the

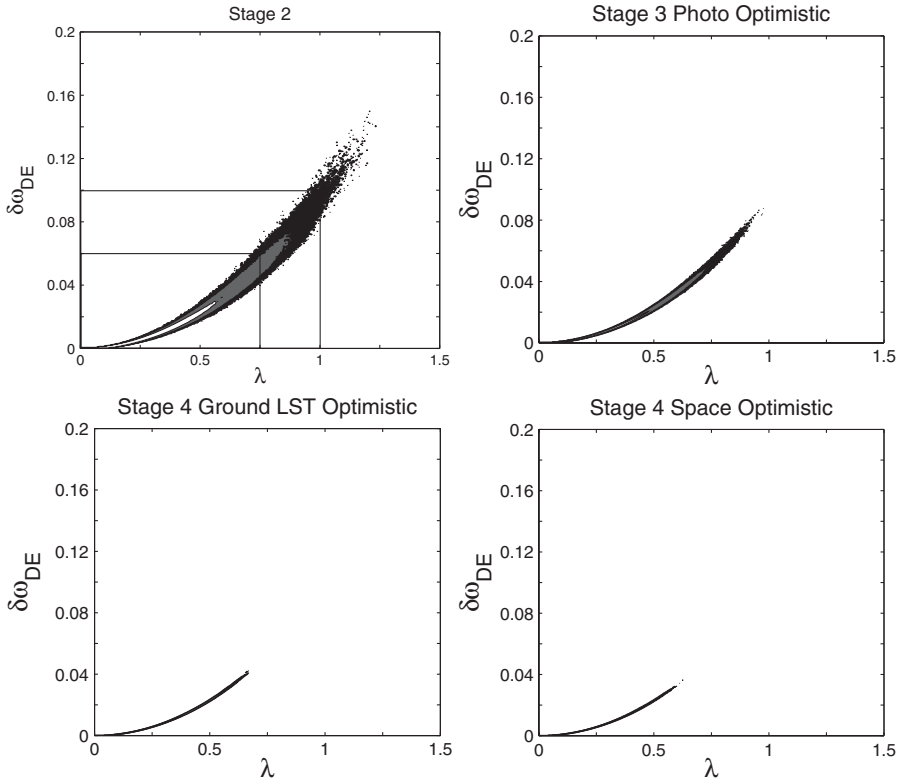

FIG. 4. Likelihood contours in the $\lambda - \delta\omega_{\rm DE}$. Deviations of $\delta\omega_{\rm DE}$ from 0 indicate evolving dark energy. The background cosmology has a cosmological constant. The boxes in the top left panel (Stage 2), respectively, show the size of the axes for Stage 3 and Stage 4 plots in Fig. 5. The contours give 68.27%, 95.44%, and 99.73% confidence regions.

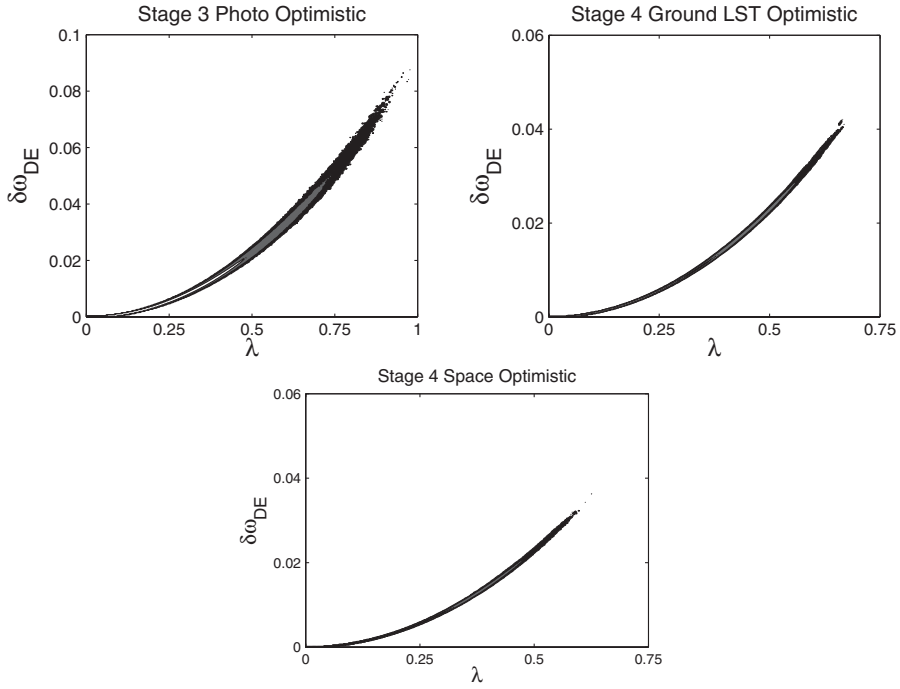

FIG. 5. Enlarged plots of the $\lambda - \delta\omega_{\mathrm{DE}}$ confidence contours for cosmological constant data models. The three contours correspond to 68.27%, 95.44%, and 99.73% confidence regions. The axes correspond to the boxes in Fig. 4.

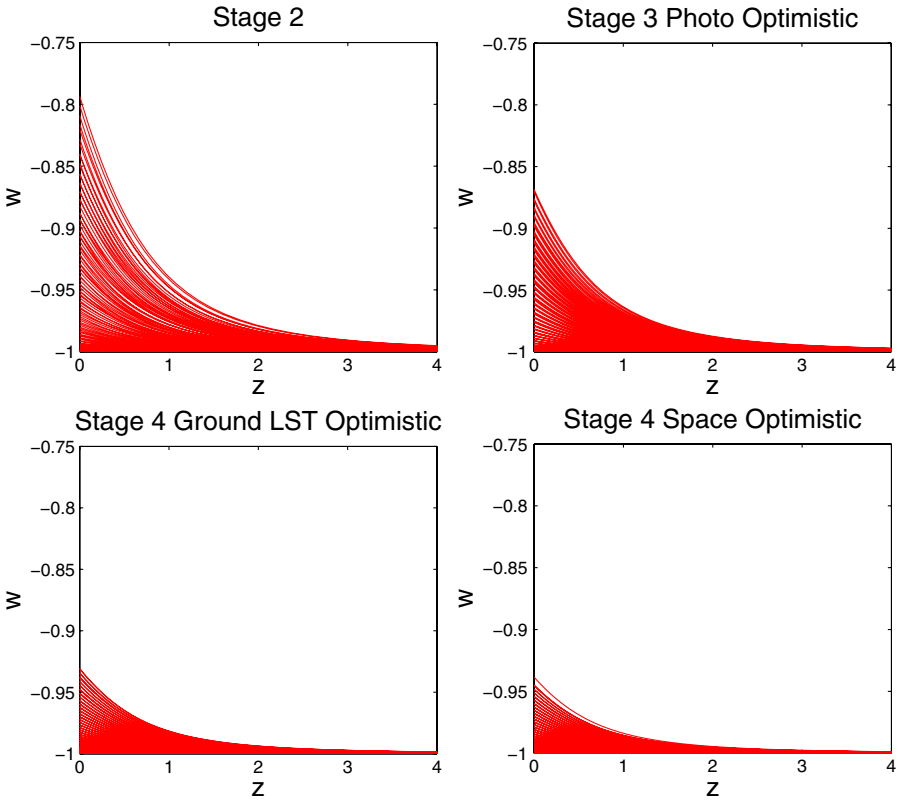

FIG. 6 (color online). The $w(z)$ behavior for a sample of points covering the full range of the $\lambda - V_I$ space for data based on a cosmological constant.

cosmological solutions vary with λ to discuss constraints on future cosmology as well. Since all the stages depicted in Fig. 3 strongly favor $\lambda < \sqrt{2}$, essentially all future $w(a)$ behavior consistent with these data sets will approach scaling solutions where $w \to \frac{\lambda^2}{3} - 1 < -\frac{1}{3}$ and give accelerating universes where $\Omega_\phi \to 1$. The scaling solutions have not been reached by today but will be approached in the future. Therefore, by Stage 2, solutions that lead to universes with a nonaccelerating fate have been ruled out in this scenario. We will revisit this point in the next section in the context of a different background cosmology.

V. EXPONENTIAL MODEL FIDUCIAL DATA

Next we consider the case where the universe happens to have dark energy described by the exponential model. We select a particular fiducial model of dark energy to illustrate the potential impact of Stage 4 data. We use exponential model parameters of $\lambda = 0.7$ and $V_I = 0.42$ for the fiducial model (the remaining parameters were given the same values we use for the cosmological constant background model, given in Table I).

We choose the fiducial values by finding a point in the $\lambda - V_I$ space in Fig. 3 for Stage 2 that was just outside a 1σ detection but was excluded by better than 3σ in Stage 4 Optimistic (for both ground and space). This point corresponds to $w(a = 1) = -0.92$, as shown in Fig. 2. The results of Stage 2, Stage 3 Photo Optimistic, Stage 4 Space Optimistic, and Stage 4 LST Optimistic are shown in Fig. 7 for the $\lambda - V_I$ space. The $\lambda - \delta\omega_{\rm DE}$ space is shown in Fig. 8. Figure 9 shows an enlarged version of the $\lambda - \delta\omega_{\rm DE}$ space for Stage 4 experiments.

For Stage 2, the likelihood contours in $\lambda - V_I$ space look similar to the case with a cosmological constant background cosmology. The range of λ is nearly the same with all $\lambda < \sqrt{2}$. Therefore the same conclusions about strongly favoring future scaling behavior that were made in the previous section apply here. The upturned trend is a little more dramatic since dark energy solutions with more evolution are favored. The major difference in the space is that values of $\lambda \lesssim 0.05$ are outside the 1σ contour. Comparing this with the 1σ region of $\delta\omega_{\rm DE}$ shows that these values are consistent with a nondynamical dark energy. It is not until we reach values of $\lambda \approx 0.2$ that we find a 1σ region that corresponds to an evolving dark energy in the $\delta\omega_{\rm DE}$ plot. Therefore, even though the parameters consistent with a cosmological constant fall outside the 1σ contour in the $\lambda - V_I$ plot, a nondynamical dark energy, and thus a cosmological constant, is not ruled out at even the 1σ level by analyzing the contours in the $\lambda - \delta w_{\rm DE}$ space. This apparent discrepancy between the two pictures is in fact a common situation when examining relatively low likelihood contours in different parameter spaces. More clear signals will only be found

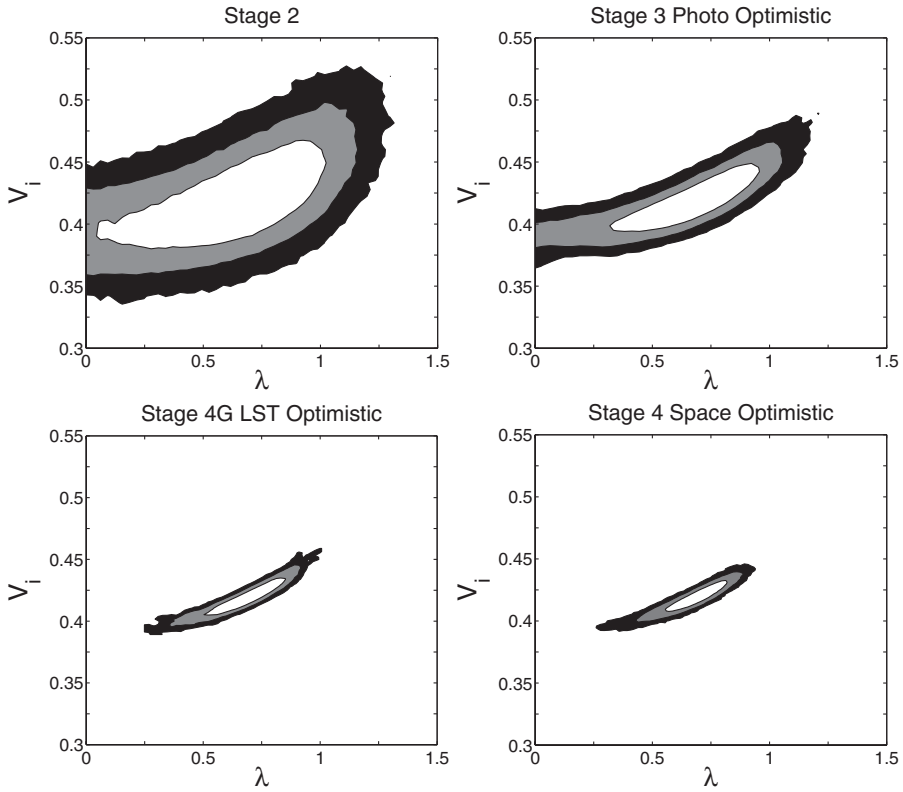

FIG. 7. Plots of the likelihood in $V_I - \lambda$ space for data based on the fiducial exponential background cosmology. The three contours correspond to 68.27%, 95.44%, and 99.73% confidence regions.

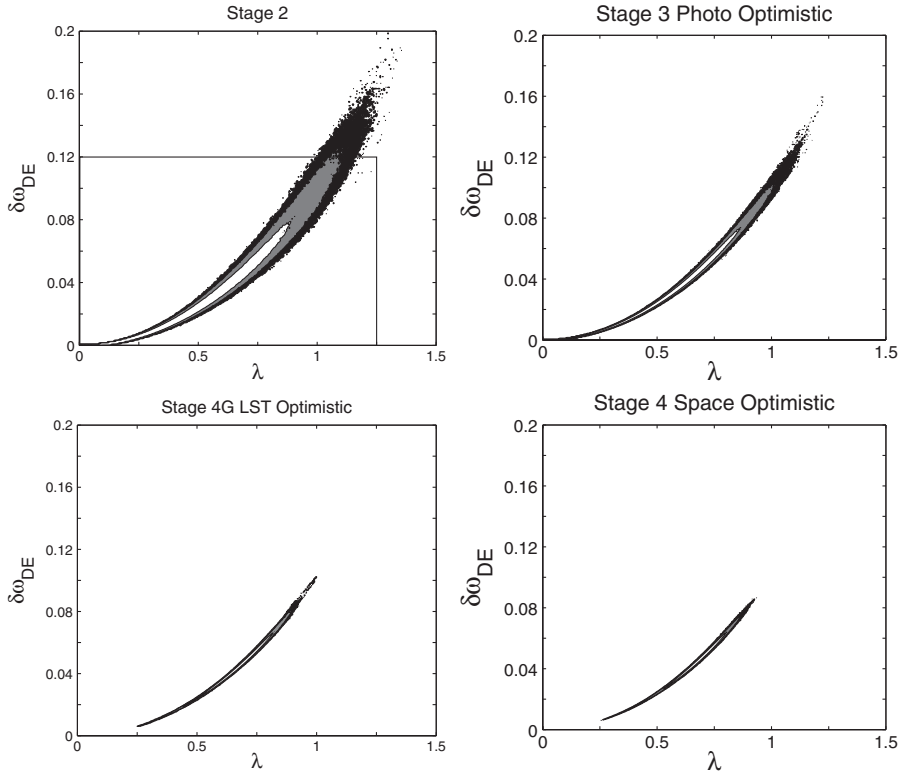

FIG. 8. Plots of the $\lambda - \delta\omega_{\rm DE}$ confidence contours for data based on the fiducial exponential background cosmology. The three contours correspond to 68.27%, 95.44%, and 99.73% confidence regions. The box in the top left figure (Stage 2) shows the size of the axes for the Stage 4 plots in Fig. 9.

when looking at phenomena that are rejected at higher likelihood levels.

By Stage 3 Photo Optimistic, the cosmological constant is now excluded in the 1σ contour although well within the 2σ contour in the $\lambda - V_I$ space. This is consistent with the $\lambda - \delta\omega_{\rm DE}$ plot in Fig. 8. The increased constraining power is again equivalent to the DETF result for the $\lambda - V_I$ space. However, the range of λ has not changed much within the 3σ contour, allowing the range of evolving dark energy solutions to be nearly as large as Stage 2, as seen in Fig. 8.

Stage 4 clearly differentiates between the exponential fiducial model and a cosmological constant by better than 3σ, as shown in both $\lambda - \delta\omega_{\rm DE}$ and $\lambda - V_I$ spaces depicted in Figs. 7 and 8. Again, the increased constraining power is consistent with the DETF results for both Stage 4 experiments.

Figure 10 shows the span of the $w(z)$ solutions for each of the stages determined in the same way as in the previous section. The curve with the greatest $w(z = 0)$ departure from -1 is obtained from the top right tip of the 3σ curve in the $\lambda - V_I$ space. For the Stage 4 plots, the bottom most curve, corresponding to the closest approach to a cosmological constant, corresponds to the bottom left tip of the 3σ region in the $\lambda - V_I$ space.

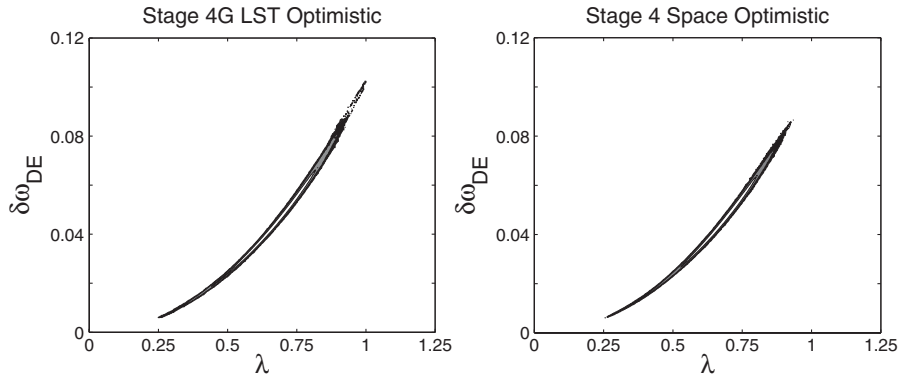

FIG. 9. Enlarged plots of the $\lambda - \delta\omega_{\rm DE}$ confidence contours for data based on an exponential model. The three contours correspond to 68.27%, 95.44%, and 99.73% confidence regions. The axes correspond to the box in Fig. 8.

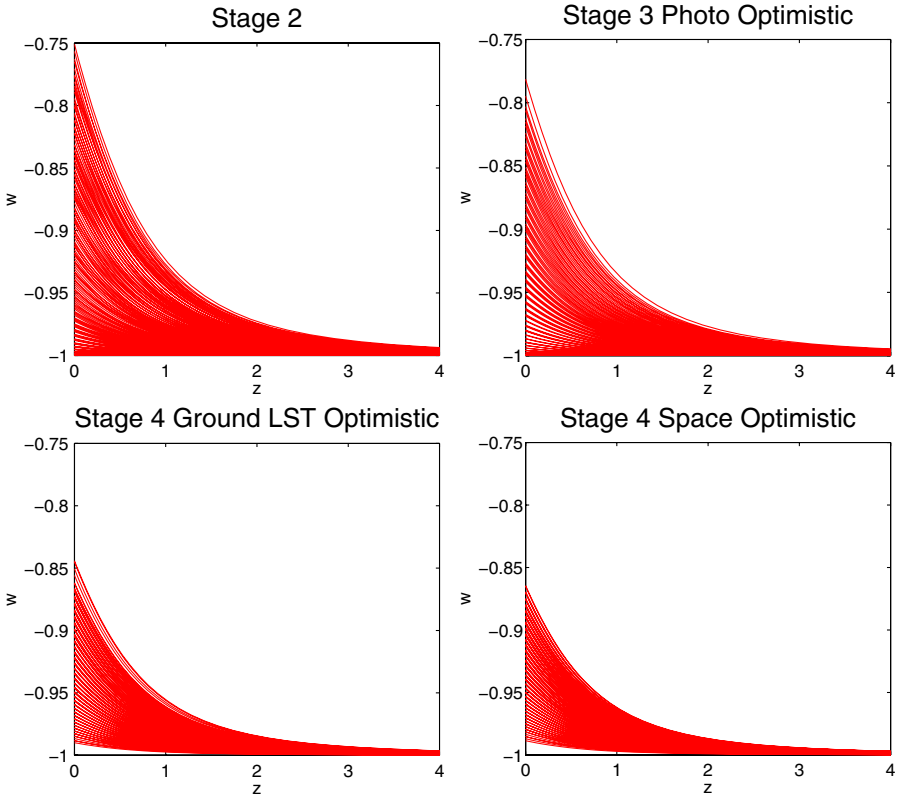

FIG. 10 (color online). The $w(z)$ behavior for a sample of points covering the full range of the $\lambda - V_I$ space for data based on an exponential model.

VI. DISCUSSION AND CONCLUSIONS

We have analyzed the exponential scalar field model using MCMC techniques for the DETF simulated data sets representing future dark energy experiments. We have demonstrated the ability of these experiments to place significant constraints on the parameters of a scalar field model. The relative constraints on the size of the $\lambda - V_I$ space between various data sets produce values similar to the constraints computed by the DETF in the $w_0 - w_a$ space. In addition to placing constraints on the quintessence parameters, we also presented our results in terms of the evolution of the dark energy in our quintessence model. This allows us to distinguish more directly between a cosmological constant and our particular scalar field model. We have presented plots for a characteristic selection of combined DETF data models, but in the course of this work we have also examined similar plots for a much wider range of DETF data models, including data models representing single techniques. We found that the consistency with constraints reported by the DETF in $w_0 - w_a$ space to hold across the entire range of data choices and combinations were considered.

We based our data on two different background cosmologies, one with a cosmological constant and one with exponential model quintessence with specific parameters. We found that the equivalence with the DETF results held in both cases. Our specific background quintessence model was chosen (with the parameter values of $V(\phi_I) = 0.42$ and $\lambda = 0.7$) in order to illustrate the power of Stage 4 experiments. For this model, the maximum deviation from $w = -1$ occurs today, with $w(a = 1) = -.92$. We found that if the universe is accelerating due to this particular exponential quintessence model then a cosmological constant dark energy model can be ruled out to at least 3σ by good Stage 4 experiments. For this background cosmology, the cosmological constant is within the 1σ contour at Stage 2 and the 2σ contour at Stage 3.

We note that there are a number of ways experiments might be optimized to do better than the cases considered by the DETF (see, for example, [16,17]). We have not included such ideas in our work, with an eye for offering more direct points of comparison with the DETF. However, improvements such as these could lead to more powerful constraints on quintessence models than we have calculated here.

We have found in this work and in our companion papers [13,14] that a wide variety of quintessence models (with widely varying families of functions $w(z)$) are constrained by DETF data in a way comparable to the constraints found in $w_0 - w_a$ space by the DETF. As discussed in [18], we believe that this is related to recent work by one of us (A. A.) and Bernstein [5], where it was demonstrated that, overall, the good DETF simulated data sets could constrain significantly more than two dark energy parameters. From this point of view our various models of

dark energy are just sampling different more or less ''random'' combinations of the ''well measured modes'' discussed in [5] and in each case are coming up with similar results.

ACKNOWLEDGMENTS

We thank Matt Auger, Lloyd Knox, and Michael Schneider for useful discussions and constructive criticism. Thanks also to Jason Dick who provided much useful advice on MCMC. We thank the Tony Tyson group for use of their computer cluster, and, in particular, Perry Gee and Hu Zhan for expert advice and computing support. Gary Bernstein provided us with Fisher matrices suitable for adapting the DETF weak lensing data models to our methods, and David Ring and Mark Yashar provided additional technical assistance. This work was supported by DOE Grant No. DE-FG03-91ER40674 and NSF Grant No. AST-0632901.

[1] A. G. Riess *et al.* (Supernova Search Team), Astron. J. **116**, 1009 (1998).
[2] S. Perlmutter *et al.* (Supernova Cosmology Project), Astrophys. J. **517**, 565 (1999).
[3] A. Albrecht *et al.*, arXiv:astro-ph/0609591.
[4] A. R. Liddle, P. Mukherjee, D. Parkinson, and Y. Wang, Phys. Rev. D **74**, 123506 (2006).
[5] A. Albrecht and G. Bernstein, Phys. Rev. D **75**, 103003 (2007).
[6] J. Dick, L. Knox, and M. Chu, J. Cosmol. Astropart. Phys. 07 (2006) 001.
[7] D. Huterer and H. V. Peiris, Phys. Rev. D **75**, 083503 (2007).
[8] J. J. Halliwell, Phys. Lett. B **185**, 341 (1987).
[9] P. G. Ferreira and M. Joyce, Phys. Rev. D **58**, 023503 (1998).
[10] P. G. Ferreira and M. Joyce, Phys. Rev. Lett. **79**, 4740 (1997).
[11] B. Ratra and P. J. E. Peebles, Phys. Rev. D **37**, 3406 (1988).
[12] E. J. Copeland, A. R. Liddle, and D. Wands, Phys. Rev. D **57**, 4686 (1998).
[13] A. Abrahamse *et al.*, preceding Article, Phys. Rev. D **77**, 103503 (2008).
[14] M. Barnard *et al.*, this issue, Phys. Rev. D **77**, 103502 (2008).
[15] We set the initial value of $\frac{d\phi}{dt}$ to zero because it simplifies the problem while still giving us an interesting set of solutions to work with. Allowing nonzero initial values of $\frac{d\phi}{dt}$ would increase the fine tuning issues without leading to a more interesting set of cosmologies.
[16] H. Zhan, J. Cosmol. Astropart. Phys. 08 (2006) 008.
[17] M. Schneider, L. Knox, H. Zhan, and A. Connolly, Astrophys. J. **651**, 14 (2006).
[18] A. Albrecht, AIP Conf. Proc. **957**, 3 (2007).